

Article

Effect of Carbon Black Nanoparticles from the Pyrolysis of Discarded Tires on the Performance of Asphalt and its Mixtures

Chuangmin Li ^{1,2}, Ziran Fan ², Shaopeng Wu ^{3,*}, Yuanyuan Li ^{3,*}, Youwei Gan ² and Aoming Zhang ⁴

¹ The Key Laboratory of Road Structure & Material Ministry of Transport, Beijing 100088, China; lichuangmin@126.com

² School of Traffic and Transportation Engineering, Changsha University of Science and Technology, Changsha 410114, China; fanziran@stu.csust.edu.cn (Z.F.); ganyouwei@stu.csust.edu.cn (Y.G.)

³ State Key Laboratory of Silicate Materials for Architectures, Wuhan University of Technology, Wuhan 430070, China

⁴ School of Civil Engineering and Architecture, Hubei University of Arts and Science, Xiangyang 441021, China; zhangam2018@163.com

* Correspondence: wusp@whut.edu.cn (S.W.); liyuanyuan@whut.edu.cn (Y.L.); Tel.: +86-27-8716-2595 (S.W.)

Received: 15 March 2018; Accepted: 13 April 2018; Published: 17 April 2018



Abstract: It is of great benefit to the environment and the economy to use discarded tires pyrolysis carbon black (TPCB) nanoparticles as a modifier for asphalt binders. A base asphalt binder with 60/80 penetration (GF-70) was selected to prepare the TPCB-modified asphalt binder (TPCB/GF-70) with a 15% dosage of TPCB by the melt blending method. The test instruments, such as Fourier transform infrared spectroscopy, laser particle size analyzer, and thermogravimetric analyzer, were used to study the characteristics of TPCB. The physical performance of GF-70 and TPCB/GF-70 were tested and the rheological properties were also tested with a dynamic shear rheometer to investigate TPCB's effect on the performance of GF-70. In addition, the aromatic hydrocarbon oil (AHO) was used as the softening agent for TPCB/GF-70. The pavement performance of AC-13 and AC-20 was studied to evaluate the comprehensive effect of TPCB and AHO on the pavement performance of asphalt mixtures. Results show that a 15% dosage of TPCB can significantly improve the anti-rutting performance of GF-70, and decrease the low-temperature performance of GF-70 within one PG grade. AHO can obviously improve the low-temperature performance of TPCB/GF-70, but does not significantly decrease the high-temperature performance. With the addition of AHO and a 0.1% higher oil aggregate ratio, TPCB tends to significantly improve the anti-rutting performance and the low-temperature performance of TPCB-modified mixtures; the moisture stability of TPCB and AHO composite modified mixtures satisfies the requirement of water stability.

Keywords: TPCB; asphalt and asphalt mixture; physical performance; rheological properties; optimization of pavement performance

1. Introduction

With the rapidly increase of automobiles and trucks, more than 1.5 billion waste tires are discarded every year [1]. This will inevitably lead to environmental pollution and resource wastage if we do not appropriately deal with waste tires. At present, four main methods are used to deal with these tires, namely pyrolysis [2,3], incineration [4], landfill [5,6], and powder manufacturing [7–9]. However, three of these four methods are accompanied by other disadvantages [10]. Pyrolysis is a pioneering method that can be used to generate carbon black, tire oil, and syngas from waste tires in the absence of oxygen.

Pyrolysis has a series of advantages, such as low cost, high efficiency, little environmental pollution, and its key product being renewable carbon black (with a mass ratio of 30% and up depending on the pyrolysis temperature) [3]. However, because of the limited usage of discarded tires pyrolysis carbon black (TPCB) nanoparticles [11], TPCB is produced and immediately accumulated. Therefore, it is very important to broaden the application range of TPCB.

In recent years, plenty of studies have been conducted to use carbon black (CB) as a modifier for asphalt binders [12–20]; these works are a good start towards enlarging the application field of CB. Previous research investigated the modified effect of CB on the workability or mechanical properties of asphalt binders and their mixtures, with the results indicating that CB had good compatibility with asphalt binders and a reinforcement effect on asphalt binders, and decreased the resistivity of asphalt [12]; it could improve the complex modulus [13] and anti-aging performance (ultraviolet aging and thermo-oxidative aging) of asphalt binders [15], as well as enhance the anti-rutting performance of asphalt mixtures at high temperatures [14]. However, there was no consistent conclusion about the effect on low-temperature performance: some studies showed that carbon black could improve the low-temperature performance of asphalt, while others showed that it cannot or that it has no effect [16,17]. However, in general, micrometer and nanometer powder materials always have a stiffening effect on asphalt and can reduce the anti-crack property of asphalt at low temperatures [18–20].

In addition, previous research mostly studied the modified effect of industrial carbon black. The performance of CB depends on its structure, surface area, and particle size. TPCB differs from industrial carbon black in terms of its composition and structure form. For example, the particle size of TPCB is roughly equal to the average particle size of industrial carbon black, which indicates that TPCB is a compound material consisting of different kinds of industrial carbon black [10]. The desorption ability of TPCB is poor [19] and may not have good compatibility with rubber or may be difficult to disperse uniformly in asphalt. The modified effects of TPCB on the performance of asphalt binders or its mixtures may be different to industrial carbon blacks, so it is of great importance to investigate the TPCB effect on the pavement performance of asphalt binders and their mixtures.

In this paper, the characteristic functional groups, particle size distribution, and thermostability of TPCB are studied. A base asphalt binder of Maoming GaoFu 60/80 asphalt binder (GF-70) was designated to prepare the TPCB-modified GF-70 (TPCB/GF-70) by mixing it with a 15% dosage of TPCB; the physical performance and rheological properties were investigated to evaluate the influence of TPCB on GF-70. In order to improve the low-temperature performance of TPCB/GF-70, four levels of dosage (0.3%, 0.6%, 0.9%, and 1.2%) of aromatic hydrocarbon oil (AHO) were used as the softening agent for TPCB/GF-70. Finally, two kinds of asphalt mixtures of AC-13 and AC-20 were created to investigate the influence of TPCB on the pavement performance of asphalt mixtures.

2. Materials and Methods

2.1. Materials

2.1.1. Asphalt Binder

A base asphalt binder of GF-70 was provided by Sinopec Maoming Company (Maoming, Guangdong, China). Table 1 gives the technical information of GF-70.

Table 1. Technical information on GF-70.

Asphalt	Technical Information	Units	Results	Requirements	Methods
Virgin	Penetration (25 °C)	0.1 mm	70.3	60~80	ASTM D5 [21]
	Softening point	°C	47.5	≥46	ASTM D36 [22]
	60 °C dynamic viscosity	Pa.s	185	≥180	ASTM D4402 [23]
	10 °C ductility	cm	45	≥15	ASTM D113 [24]
After RTFOT	Mass loss	%	−0.18	±0.8	ASTM D2872 [25]
	25 °C residual penetration ratio	%	65.7	≥61	ASTM D5
	10 °C Residual ductility	cm	9.0	≥6	ASTM D113

2.1.2. Discarded Tires Pyrolysis Carbon Black (TPCB)

The TPCB used in this research was manufactured by Kimkey Environmental S&T Co., Ltd. (Shanghai, China). The appearance of TPCB is shown in Figure 1. Technical information on TPCB is listed in Table 2.

Table 2. Technical information on TPCB.

Technical Information	Units	Results	
Chemical data	Iodine absorption value	g/kg	81
	PH value	-	6.5
	45 μm mesh	ppm	68
	Heating loss	%	2.4
Tensile properties (145 °C, 30 min)	Elongation at break	%	565.2
	Tensile strength	MPa	25.8
Hardness	Shore hardness	%	60.0

**Figure 1.** Appearance of TPCB.

2.1.3. Softening Agent

In order to increase the low-temperature performance of TPCB modified asphalt binder, AHO was used as the softening agent to soften asphalt binder. AHO was manufactured by Hubei Guochuang Hi-tech Material Co., Ltd. (Hubei, China). AHO is a black sticky liquid, the main components of which are aromatics and colloid. It can be dissolved in asphalt to improve the component of an asphalt. At the same time, it can also increase the ductility of modified asphalt, especially at low temperatures.

2.1.4. Aggregate and Filler

The crushed basalt was used as the aggregate of the asphalt mixture. In order to ensure the stability of the granular gradation, both the coarse and fine aggregate were sieved and divided into grades. The technical information on the aggregates is shown in Table 3. It should be noticed that the aggregate was first mixed according to the aggregate gradation of the AC-20 mixture (given in the following section of this paper), then divided into coarse and fine aggregates with a diameter bigger or

smaller than 4.75 mm, respectively. The limestone powder was used as the filler of the asphalt mixture; there was no moisture and clumping phenomenon in limestone powder, the technical information for which is also given in Table 3.

Table 3. Technical information on aggregates and filler.

Aggregate	Technical Information	Results	
Coarse aggregate	Crushed stone value	14.7%	
	Los Angeles abrasion loss	21.8%	
	Percentage passing 0.075 mm sieve by washed-sieve analysis	0.18%	
	Soundness	10%	
	Water absorption	1.4%	
	Polished stone value	44.7%	
	Affinity grade with asphalt	4 grade	
Fine aggregate	Clay content (percentage passing 0.075 mm sieve)	1.1%	
	Soundness	11%	
	Sand equivalent value	60.9%	
Filler	Apparent density	2.694 g/m ³	
	Hydrophilic coefficient	0.84	
	Plasticity index	3.0	
	Gradation by percentage of mass passing sieve size	<0.60 mm	100%
		<0.15 mm	94.8%
<0.075 mm		82.0%	

2.2. Preparation of TPCB-Modified Asphalt

The preparation procedure of TPCB-modified asphalt was as follows: first, neat asphalt was heated to a constant temperature of 155 °C; then a 15% dosage of TPCB was added to the neat asphalt (mass ratio of TPCB to neat asphalt); finally, a high-speed shearing machine was used for 40 min with a shear temperature of 155 °C and shear rate of 4000 r/min.

TPCB and AHO compound modifier modified asphalt was produced as follows: GF-70 was heated to a constant temperature of 155 °C, the designed dosages of AHO and TPCB were added to neat asphalt, and a high-speed shearing machine was used for 45 min, with a shear temperature of 155 °C and a shear rate of 4000 r/min.

2.3. Experiments on TPCB

2.3.1. Chemical Structure Testing of TPCB

The characteristic functional groups of TPCB were tested by a Fourier transform infrared (FTIR) spectrometer. The potassium bromate (KBr) disk method was used to prepare the TPCB samples for FTIR testing, with a mass ratio of TPCB to KBr of 1 mg/100 mg. The instrument parameters of FTIR were that the scan time was set to 64 times, and scan wave number range was 4000 cm⁻¹~400 cm⁻¹.

2.3.2. Laser Size Analysis Testing of TPCB

The laser particle size analyzer, produced by Jinan Micronano Particle Instrument Co., Ltd. (Jinan, Shandong, China), was used to investigate the particle size distribution of TPCB. The particle size test range of this instrument was from 1 nm to 10,000 nm; the dispersible agent was alcohol with a viscosity of 0.001096 Pa·s, the refractive index was 1.332, and the delay unit time was 50 μs.

2.3.3. Thermogravimetric Testing of TPCB

The thermal properties of TPCB were investigated by thermogravimetric (TG) testing in air, with the test temperature range from 50 °C to 700 °C, the heating rate at 10 °C/min, and the mass of every sample at 10 mg.

2.4. Experiments on Asphalt

2.4.1. Physical Properties of Asphalt

Penetration testing was done according to the criterion of ASTM D5 at three temperatures, 15, 25, and 30 °C; other parameters such as PI, equivalent softening point (T_{800}), and equivalent brittle point ($T_{1.2}$) were calculated according to Equations (1)–(3), respectively. The softening point and ductility of GF-70 and TPCB/GF-70 were investigated depending on the criteria of ASTM D36 and ASTM D113, respectively.

$$PI = \frac{20(1 - 25A)}{1 + 50A} \quad (1)$$

$$T_{800} = \frac{\lg_{800} - K}{A} = \frac{2.9031 - K}{A} \quad (2)$$

$$T_{1.2} = \frac{\lg_{1.2} - K}{A} = \frac{0.0792 - K}{A}, \quad (3)$$

where A and K are the slope and intercept of the linear regression equation of the logarithm of penetration at three different temperatures, 15 °C, 25 °C, and 30 °C.

2.4.2. Storage Stability Testing of Asphalt

First, the TPCB-modified asphalt was poured into an aluminum tube with a diameter and height of 25 mm and 140 mm, respectively. Then, we set the aluminum tube in an oven at a constant temperature of 163 °C for 48 h and cooled it in a refrigerator at 5 °C for more than 4 h. After that, the tubes were cut into three equal sections. The softening points of the top and bottom sections were tested to calculate the softening point differences.

2.4.3. Thermal Oxide Aging Testing

A short-term aging test was conducted, the rolling thin film oven test (RTFOT), at a temperature of 163 ± 0.5 °C for 85 min, according to the criterion of ASTM D2872. The long-term aging test was conducted by the pressure aging vessel (PAV) method at a temperature of 100 ± 0.5 °C for 20 h, according to the criterion of ASTM D6521-08.

2.4.4. Rheological Properties Testing

The rheological properties of both GF-70 and TPCB/GF-70, not aged by RTFOT and PAV, were investigated by a dynamic shear rheometer (DSR) in the temperature range from -10 °C to 85 °C; the frequency was 10 rad/s. In the temperature range from -10 °C to 30 °C, a rotor with a diameter of 8.0 mm was used, the thickness of the sample was 2.0 mm, and the strain was 0.05%; the rotor with a diameter of 25 mm was used in the temperature range from 30 °C to 85 °C, where the thickness of the sample was 1.0 mm and the strain was 0.5%.

2.4.5. BBR Testing

Before the bending beam rheometer (BBR) test, the asphalt binder was first aged by RTFOT, followed by PAV. The BBR test was conducted at a temperature of -12 °C and -18 °C, respectively, to investigate the TPCB effect on the low-temperature creep properties of GF-70. The sample size of asphalt binder beams for the BBR test was 125 mm \times 12.5 mm \times 6.25 mm, the binder beams were set to an absolute ethanol bath at the experiment temperature for 60 ± 5 min, then, the creep stiffness and m -values of asphalt binders were tested with a constant load of 980 ± 50 mN for 240 s.

2.5. Experiments on the Asphalt Mixture

Wheel tracking testing was done to study the anti-rutting performance of asphalt mixtures, where the test temperature was 60 °C and the load was 0.7 MPa; a low-temperature bending test was

performed to detect the anti-crack performance and strain of asphalt mixtures at $-10\text{ }^{\circ}\text{C}$ with a loading rate of 50 mm/min . The study of water stability was mainly based on an immersion Marshall test and the freeze–thaw split test. The immersion Marshall test was undertaken in a water bath for 48 h at a constant temperature of $60\text{ }^{\circ}\text{C}$. Marshall stability was named “normal Marshall stability” (MS_1) before this test and “condition Marshall stability” (MS_2) after this test. The conditions for the freeze–thaw split test were freezing for 16 h at $-18\text{ }^{\circ}\text{C}$, followed by a water bath at $60\text{ }^{\circ}\text{C}$ for 24 h; splitting tensile strength was named “normal splitting tensile strength” (ST_1) before this test and “condition splitting tensile strength” (ST_2) after this test. The residential Marshall stability (RMS) and splitting tensile strength ratio (TSR) were calculated according to Equations (4) and (5):

$$\text{RMS} = \frac{MS_2}{MS_1} \times 100 \quad (4)$$

$$\text{TSR} = \frac{ST_2}{ST_1} \times 100, \quad (5)$$

where MS_1 (MPa) is the normal Marshall stability; MS_2 (MPa) is the condition Marshall stability; RMS (%) is the ratio of MS_1 to MS_2 ; ST_1 (MPa) is the normal splitting tensile strength; ST_2 (MPa) is the condition splitting tensile strength; and TSR (%) is the ratio of ST_1 to ST_2 .

3. Results and Discussion

3.1. Characterization of TPCB

3.1.1. Chemical Structure of TPCB

Figure 2 shows the FTIR spectrum of TPCB. Because of the simple graphite-like molecular structure of TPCB, most of the chemical bonds in TPCB are non-polar bonds. The infrared activity non-polar bonds are very weak [26,27], so the FTIR spectrum is simple, with four different absorption bands. The relatively wide domain absorption band at 3438 cm^{-1} is caused by the stretching vibration of $-\text{OH}$ of H_2O , because TPCB can absorb water from the air. The absorption bands at 1450 cm^{-1} and 1604 cm^{-1} [28,29] are assigned to the stretching vibration of the sp^2 hybrid $\text{C}=\text{C}$, which is caused by the carbon atoms in the graphite-like sheets of TPCB. The absorption band at 1104 cm^{-1} is caused by the stretching vibration of $\text{C}-\text{O}$ [30], which is due to the structural defects (sp^3 hybrid carbon atoms) in the graphite-like structures.

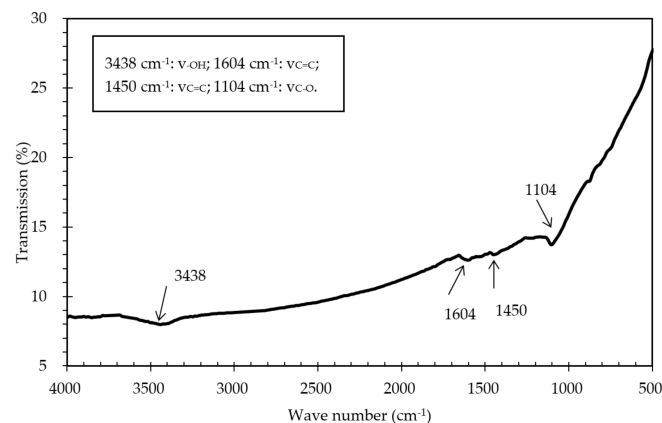


Figure 2. FTIR spectrum of TPCB.

3.1.2. Particle Size Distribution of TPCB

The particle size distribution of TPCB was investigated by laser size analysis. The curves corresponding to the Gaussian fit are shown in Figure 3. The size of TPCB nanoparticles is mainly

distributed in the diameter range from 50 nm to 5000 nm. In detail, the D_{10} (accumulation of 10%), D_{50} (accumulation of 50%) and D_{90} (accumulation of 90%) of TPCB are 200.35 nm, 481.65 nm, and 1159.35 nm, respectively, which indicates that the particle size distribution of TPCB is not uniform. The reason is that, on the one hand, in order to satisfy the requirements of characteristics at different positions of tires, different kinds of CB are added to the tires, so that TPCB is a compound of different kinds of CB from the raw material of tires; on the other hand, the coking substances generated in the pyrolysis process can affect the particle size distribution of TPCB.

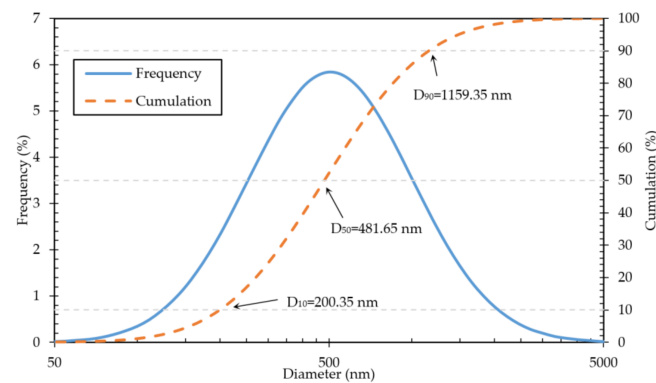


Figure 3. The Gaussian fit of laser size analysis of TPCB.

3.1.3. Thermal Properties of TPCB

The thermogravimetric (TG), differential thermogravimetric (DTG), and differential scanning calorimetric (DSC) curves are shown in Figure 4 to study the thermal properties of TPCB. There are two mass loss stages in the TG image of TPCB. In detail, the temperature range of stage one is from 50 °C to 126 °C, the mass loss ratio in this stage is 1.42%, and the fastest loss rate can be found at a temperature of 94.3 °C. The peak value of 102.9 °C in the DSC curve shows that stage one is an endothermic phase, so it corresponds to the endothermic phase of the evaporation of water by TPCB. The temperature range of stage two is from 126 °C to 700 °C. There is a peak value of 416.4 °C in the DSC curve, which indicates that stage two is a heat-releasing phase and mainly corresponds the combustion of the residual organics in TPCB. The mass loss ratio of 10.38% is relatively larger in this stage, but the heating temperature in the preparation process of TPCB/GF-70 is not higher than 160 °C and the mass loss ratio at 160 °C is only 2.76%, which shows that the thermal properties of TPCB can satisfy the requirements for preparing a TPCB-modified asphalt binder.

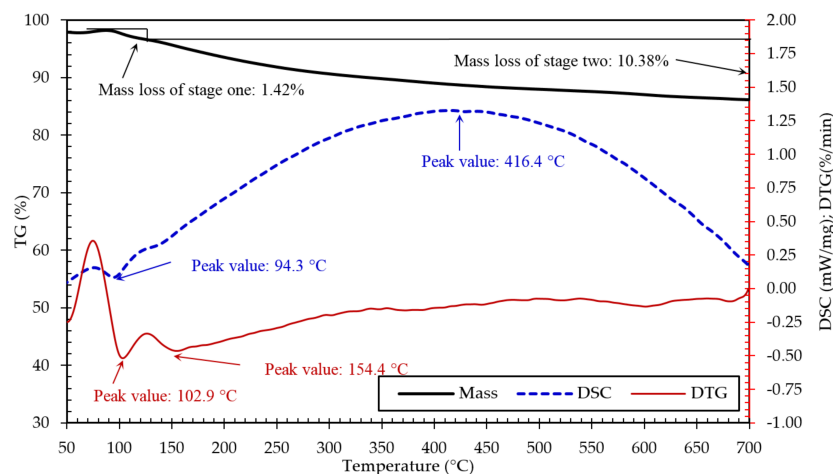


Figure 4. TG, DTG, and DSC curves of TPCB in the temperature range of 50 °C to 700 °C.

3.2. TPCB's Effect on the Performance of Asphalt

3.2.1. TPCB's Effect on the Physical Performance of Asphalt

The physical performance of GF-70 and TPCB/GF-70 asphalt binders is shown in Table 4. The penetration, softening point, ductility, and segregation test results of TPCB/GF-70 all meet the requirements of AH-70 B grade in China [31].

Table 4. Results of physical performance and segregation tests of GF-70 and TPCB/GF-70.

Asphalt	25 °C Penetration (0.1 mm)	Softening Point (°C)	10°C Ductility (cm)	PI	T ₈₀₀ (°C)	T _{1.2} (°C)	Softening Point Difference (°C)
GF-70	70.3	47.5	45.0	−0.44	48.9	−21.5	-
TPCB/GF-70	59.4	50.4	18.7	−0.29	51.7	−15.8	0.7

Penetration, softening point, and T₈₀₀ are able to reflect the high-temperature performance of an asphalt binder: the lower the penetration, and the higher the T₈₀₀ and softening point, the better the high-temperature performance [32]. The penetration of GF-70 decreases by 15.5% with the addition of a 15% dosage of TPCB, while the softening point and T₈₀₀ increase by 2.9 °C and 2.8 °C, respectively, which shows that TPCB can improve the high-temperature performance of asphalt.

The ductility and T_{1.2} belong to the indexes for evaluating the low-temperature performance of an asphalt binder. After adding TPCB, the ductility decreases by 58.4% and the T_{1.2} increases by 5.7 °C, which shows that the 15% dosage of TPCB can obviously decrease the low-temperature performance of asphalt.

The PI can reflect the temperature sensitivity of an asphalt binder: the higher the PI, the lower the temperature sensitivity. In general, the PI of a sol-gel asphalt binder should be in the range of −2~2. It can be seen from Table 4 that the PI of both GF-70 and TPCB/GF-70 belong to the sol-gel asphalt binders. The PI of TPCB/GF-70 is bigger than that of GF-70; therefore, TPCB can decrease the temperature sensitivity of asphalt.

The softening point difference of segregation test is 0.7 °C, which shows that a 15% dosage of TPCB-modified asphalt has good storage stability, and TPCB has good compatibility with asphalt.

3.2.2. TPCB's Effect on the Rheological Properties of Asphalt

(1) Complex Modulus and Phase Angle

An asphalt binder must have enough elasticity to satisfy the requirements of anti-rutting at high temperatures, while having enough plasticity to avoid cracks at low temperatures. The viscoelastic properties of the asphalt binder are important to the pavement performance of asphalt mixtures [33–35]. In order to study the TPCB effect on the rheological properties of GF-70, the complex modulus (G^*) and phase angle (δ) of asphalt binders without and with TPCB were studied by the DSR. The parameter G^* can estimate the deformation resistance of an asphalt binder under repeated shear loading, and δ can reflect the ratios of the elastic and viscous characteristics of an asphalt binder [36,37]. G^* and δ of asphalt binders without and with TPCB are shown in Figure 5.

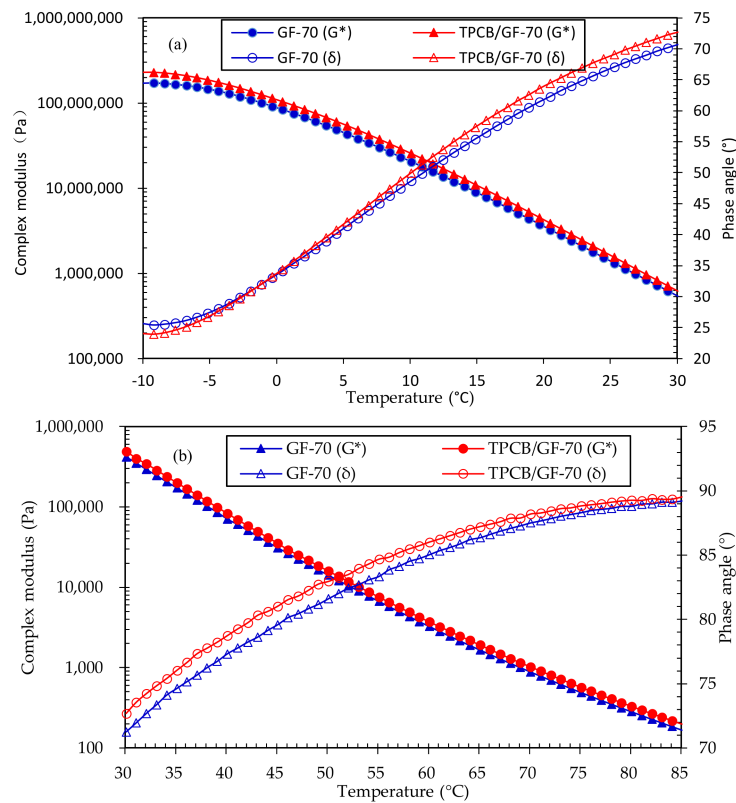


Figure 5. G^* and δ of GF-70 and TPCB/GF-70 in the temperature range of $-10\sim 30\text{ }^\circ\text{C}$ (a) and $30\sim 85\text{ }^\circ\text{C}$ (b).

It can be seen from Figure 5 that the G^* of TPCB/GF-70 is bigger than that of GF-70 in the temperature range $-10\sim 30\text{ }^\circ\text{C}$, and the same tendency can be observed in the temperature range $30\sim 85\text{ }^\circ\text{C}$, indicating that a 15% dosage of TPCB can improve the repeated shear deformation resistance of GF-70. From Figure 5a, when the temperature is lower than $0\text{ }^\circ\text{C}$, the δ of TPCB/GF-70 is smaller than that of GF-70; when the temperature is higher than $0\text{ }^\circ\text{C}$, the opposite occurs. From Figure 5b, the δ of TPCB/GF-70 is bigger than that of GF-70 in the temperature range $30\sim 85\text{ }^\circ\text{C}$, which shows that the elastic characteristic of TPCB/GF-70 is more obvious than that of GF-70 when the temperature is lower than $0\text{ }^\circ\text{C}$; the viscous ratio of G^* of TPCB/GF-70 is higher than that of GF-70 when the temperature is higher than $0\text{ }^\circ\text{C}$.

(2) Rutting Factor and Fatigue Factor

The rutting factors ($G^*/\sin\delta$) of GF-70 and TPCB/GF-70 are shown in Figure 6a. The higher the $G^*/\sin\delta$, the better the high-temperature anti-rutting performance of an asphalt binder. The $G^*/\sin\delta$ of TPCB/GF-70 is higher than that of GF-70 in the high-temperature range of $52\text{ }^\circ\text{C}\sim 82\text{ }^\circ\text{C}$, indicating that a 15% dosage of TPCB can improve the anti-rutting performance of GF-70. In order to ensure an asphalt binder has good rutting resistance, the $G^*/\sin\delta$ before aging should not be lower than 1.0 kPa. When the temperature is $69.1\text{ }^\circ\text{C}$, the $G^*/\sin\delta$ of GF-70 is 1.0 kPa, while the $G^*/\sin\delta$ of TPCB/GF-70 is 1.0 kPa at a temperature of $70.3\text{ }^\circ\text{C}$, which is $1.2\text{ }^\circ\text{C}$ higher than that of GF-70. So the high-temperature performance of TPCB/GF-70 is better than that of GF-70.

The fatigue factors ($G^*\sin\delta$) of GF-70 and TPCB/GF-70 are shown in Figure 6b. The lower the $G^*\sin\delta$, the better the anti-fatigue cracking performance of an asphalt binder. The $G^*\sin\delta$ of GF-70 becomes higher after being mixed with a 15% dosage of TPCB in the middle temperature range of $19\sim 40\text{ }^\circ\text{C}$, so that when the temperature is $22\text{ }^\circ\text{C}$, the $G^*\sin\delta$ of TPCB/GF-70 is 19.6% higher than that of GF-70, indicating that TPCB can decrease the anti-fatigue cracking performance of GF-70.

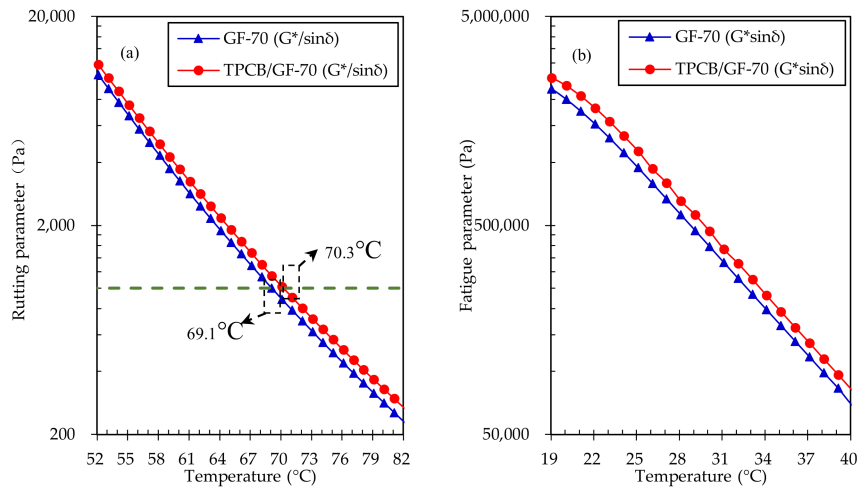


Figure 6. $G^*/\sin\delta$ (a) and $G^*\sin\delta$ (b) of GF-70 and TPCB/GF-70.

(3) Stiffness and m-Value

The low-temperature creep properties of GF-70 and TPCB/GF-70 were investigated by BBR testing, and the creep stiffness and m-values were recorded at 60 s. In order to ensure that asphalt binders have good low-temperature performance to anti-cracking, AASHTO M 320 requires that the stiffness not be higher than 300 MPa, and the m-value should not be lower than 0.300. The stiffness and m-value results of GF-70 and TPCB/GF-70 are shown in Figure 7; meanwhile, the temperatures correspond to the stiffness of 300 MPa and the m-value of 0.300 are shown in Table 5.

From Figure 7, the stiffness and m-values of GF-70 and TPCB/GF-70 satisfy the requirement of anti-cracking performance at a temperature of $-12\text{ }^\circ\text{C}$, but do not satisfy it at a temperature of $-18\text{ }^\circ\text{C}$, which shows that the low-temperature PG grade of both GF-70 and TPCB/GF-70 is $-22\text{ }^\circ\text{C}$. In detail, from Table 5, the critical low temperature of GF-70 and TPCB/GF-70 based on stiffness is $-24.4\text{ }^\circ\text{C}$ and $-22.6\text{ }^\circ\text{C}$, respectively, and the critical low temperature of GF-70 and TPCB/GF-70 based on m-value is $-24.2\text{ }^\circ\text{C}$ and $-22.6\text{ }^\circ\text{C}$, respectively, which shows that the critical low temperature of TPCB/GF-70 is $1.6\text{ }^\circ\text{C}$ higher than that of GF-70. Therefore, TPCB can decrease the anti-cracking performance of GF-70, and a 15% dosage of TPCB has an effect on the low-temperature performance of GF-70 within one PG grade.

Table 5. Temperature of stiffness is 300 MPa and m-value is 0.300.

Asphalt	Unit	Critical Low Temperature Based on Stiffness	Critical Low Temperature Based on m-Value
GF-70	$^\circ\text{C}$	-24.4	-24.2
TPCB/GF-70	$^\circ\text{C}$	-22.6	-22.6

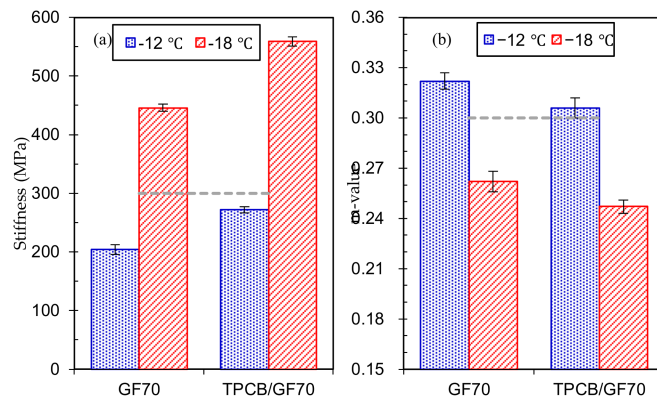


Figure 7. Stiffness (a) and m-value (b) of GF-70 and TPCB/GF-70.

3.3. Optimizing the Physical Performance of TPCB/GF-70

The results above show that TPCB can decrease the low-temperature performance of GF-70; therefore, AHO at four different dosages (0.3%, 0.6%, 0.9%, and 1.2%) was tested to investigate whether it can improve the low-temperature performance of TPCB/GF-70. The penetration, ductility, softening point, PI, T_{800} , and $T_{1.2}$ results are shown in Table 6.

From Table 6, with the addition of AHO, low-temperature indicators such as ductility and $T_{1.2}$ show a good tendency. In detail, when the dosages of AHO are 0.3%, 0.6%, 0.9%, and 1.2%, the ductility of TPCB/GF-70 increases by 3.2%, 15.5%, 27.3%, and 41.2%, respectively, while the $T_{1.2}$ decreases by 0.6%, 1.3%, 2.1%, and 2.9%, respectively. Thus, AHO can significantly improve the low-temperature anti-cracking performance of TPCB-modified asphalt, and the improvement effect is more pronounced with the increase in AHO dosage. AHO can also affect the high-temperature performance of TPCB-modified asphalt: the softening point and T_{800} decrease with the addition of AHO, and the penetration increases. However, the softening point and T_{800} of TPCB/GF-70 only decrease by 1.5 °C and 1.3 °C with a 1.2% dosage of AHO, respectively, and the high-temperature performance of TPCB/GF-70 does not obviously decrease; the softening point and T_{800} of TPCB/GF-70 are still 1.4 °C and 1.5 °C higher than that of GF-70, respectively. The PI of TPCB/GF-70 increases with the addition of AHO, which shows that the temperature sensitivity of TPCB/GF-70 decreases. In other words, AHO can obviously improve the low-temperature performance of TPCB/GF-70, but does not significantly decrease the high-temperature performance of the asphalt binder.

Table 6. AHO’s effect on the performance of TPCB/GF-70.

Dosage of AHO (%)	Penetration (100 g, 5 s, 0.1 mm)			Ductility (cm)	Softening Point (°C)	PI	T_{800} (°C)	$T_{1.2}$ (°C)
	30 °C	25 °C	15 °C					
	0	100.3	59.4					
0.3	104.3	63.4	24.6	19.3	49.8	−0.28	51.3	−16.4
0.6	105.9	67.5	25.5	21.6	49.5	−0.23	51.1	−17.1
0.9	110.4	71.3	26.9	23.8	49.1	−0.18	50.8	−17.9
1.2	115.6	75.9	28.4	26.4	48.9	−0.15	50.4	−18.7

3.4. TPCB’s Effect on the Pavement Performance of an Asphalt Mixture

3.4.1. Mix Ratio of Mixtures

Commonly used mixtures, AC-13 and AC-20, were used to study TPCB’s effect on the performance of asphalt mixtures. AC-13 was selected to represent the mixture used for the surface layer, while AC-20 represented the mixture used for middle and base layers. The GF-70 asphalt with 15% TPCB

and 1.2% AHO was used as the binder of asphalt mixtures and the optimal oil aggregate ratios of asphalt mixtures were determined according to the Marshall test. The aggregate gradation and optical oil aggregate ratio are given in Tables 7 and 8, respectively. The oil aggregate ratios of asphalt mixtures with TPCB-modified asphalt are 0.1% higher than those of asphalt mixtures without TPCB.

Table 7. Aggregate gradation of AC-13 and AC-20 mixtures.

Mixture	Passing Ratio of Every Mesh (%)											
	26.5	19	16	13.2	9.5	4.75	2.36	1.18	0.6	0.3	0.15	0.075
AC-13	100	100	100	95.2	80.4	53.2	36.9	25.8	17.2	11.5	8.1	6.4
AC-20	100	93.6	84.3	71.4	61.2	41.8	29.4	21.8	15.2	10.0	7.2	5.7

Table 8. Optical oil aggregate ratio of GF70 and TPCB/GF70 asphalt mixtures.

Mixtures	Asphalt	Optical Oil Aggregate Ratio (%)
AC-20	GF70	4.5
	TPCB/GF70	4.6
AC-13	GF70	5.1
	TPCB/GF70	5.2

3.4.2. High-Temperature Performance

The dynamic stability (DS) and rutting depth of GF70 and TPCB/GF70 asphalt mixtures were tested by a wheel tracking test to evaluate TPCB's and AHO's effects on the high-temperature performance of asphalt mixtures. Figure 8 illustrates the DS and rutting depths of GF70 and TPCB/GF70 asphalt mixtures.

It can be seen from Figure 8 that the DS values of TPCB/GF70 asphalt mixtures are all higher than those of GF70 asphalt mixtures, while the rutting depths of TPCB/GF70 asphalt mixtures are all smaller than those of GF70 asphalt mixtures. In detail, with the addition of 15% dosage of TPCB, the DS of the AC-13 mixture increases by 31.8% and the rutting depth decreases by 29.8%; the DS of AC-20 mixture increases by 27.2% and the rutting depth decreases by 14.8%. The higher the DS, and the smaller the rutting depth, the better the anti-rutting performance of the asphalt mixture. Therefore, TPCB can improve the anti-rutting performance of asphalt mixtures, and the improvement effect of TPCB on AC-13 mixture is more obvious than that of the AC-20 mixture. The enhanced effect of TPCB on the high-temperature performance of GF70 asphalt mixture can be explained in two ways: one reason is that TPCB is a kind of inorganic nanoparticle that has a hardening effect on GF70 and decreases the temperature sensitivity of GF-70, so GF-70 tends to be harder after being modified by TPCB; the other reason is that the TPCB has a large specific surface area, so needs more asphalt binder to cover its surface. The free asphalt content in mixtures decreases while the structural asphalt contents increase; as a result, the high-temperature performance of asphalt mixtures is enhanced.

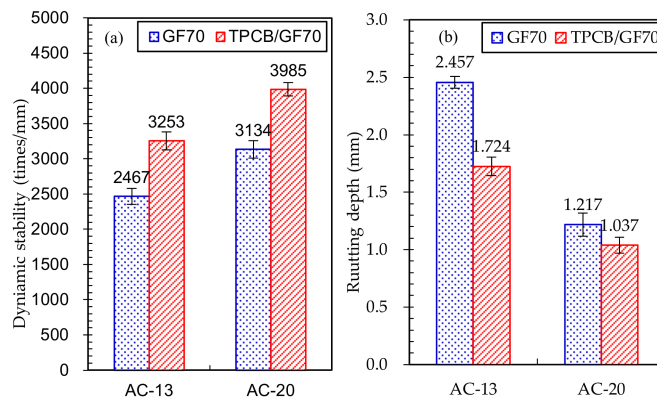


Figure 8. DS (a) and rutting deeps (b) of GF70 and TPCB/GF70 asphalt mixtures.

3.4.3. Low-Temperature Performance of Mixture

In order to investigate the TPCB and AHO effect on the low-temperature anti-cracking performance of asphalt mixtures, the flexural strength, flexural strain, and flexural modulus were tested with a low-temperature bending test. Figure 9 gives the results of a low-temperature bending test of GF70 and TPCB/GF70 asphalt mixtures.

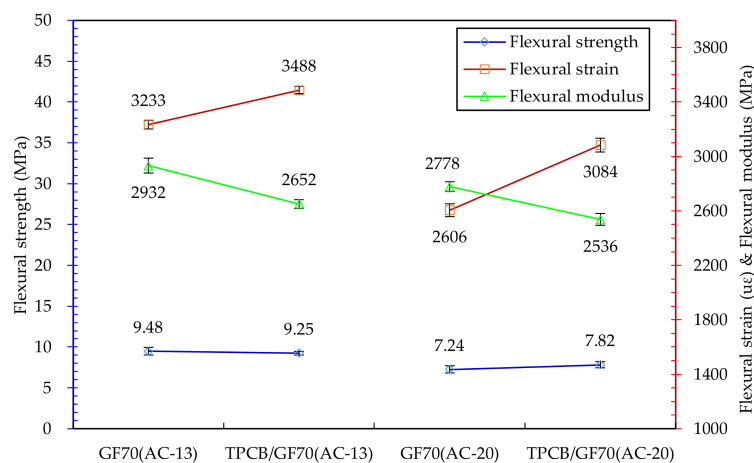


Figure 9. Results of low-temperature bending test of GF70 and TPCB/GF70 asphalt mixtures.

From Figure 9, we see that the AC-13 mixture has a larger flexural strain than the AC-20 mixture. Because of the softening effect of the 1.2% dosage of AHO and 0.1% higher oil aggregate ratio, the flexural strain experienced by the TPCB/GF70 asphalt mixtures is much greater than that of the GF70 asphalt mixtures, and the flexural moduli of TPCB/GF70 asphalt mixtures are lower than those of the GF70 asphalt mixtures. The flexural strain of the AC-13 mixture with TPCB is 7.9% larger than that of the AC-13 mixture without TPCB, and the flexural strain of the AC-20 mixture with TPCB is 18.3% bigger than that of the AC-13 mixture without TPCB. So it is feasible to improve the low-temperature performance of TPCB-modified mixtures by adding AHO and only a 0.1% higher oil aggregate ratio.

3.4.4. Water Stability of Mixture

The immersion Marshall test and freeze–thaw split test were conducted to evaluate TPCB’s and AHO’s effect on the water stability of asphalt mixtures; the bigger the RMS and TRS, the better the water stability of the asphalt mixtures [38]. Figure 10 gives the results of immersion Marshall tests of GF-70 and TPCB/GF-70 asphalt mixtures: MS₁ values of TPCB/GF-70 asphalt mixtures are all bigger than those of GF-70 asphalt mixtures; MS₂ values of GF-70 and TPCB/GF-70 asphalt mixtures

are almost equal; RMS values decrease with the addition of TPCB—AC-13 and AC-20 mixtures are decreased by 8.2% and 5.1%—but the RMS of the AC-13 mixture with TPCB is still greater than 85%, and the AC-20 mixture is still greater than 80%.

Figure 11 gives the results of freeze–thaw split tests of GF-70 and TPCB/GF-70 asphalt mixtures. Before the freeze–thaw cycle, TPCB can improve the splitting strength of a mixture; after the freeze–thaw test, the TRS of a mixture with TPCB is significantly decreased. However, the TRS of the AC-13 mixture with TPCB is still greater than 80%, and for the AC-20 mixture it is greater than 75%. So, TPCB tends to decrease the moisture stability of mixtures, but still satisfies the requirements.

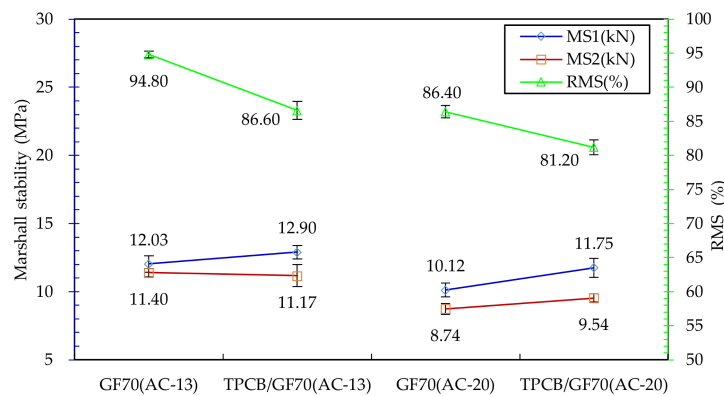


Figure 10. Results of immersion Marshall testing of GF70 and TPCB/GF70 asphalt mixtures.

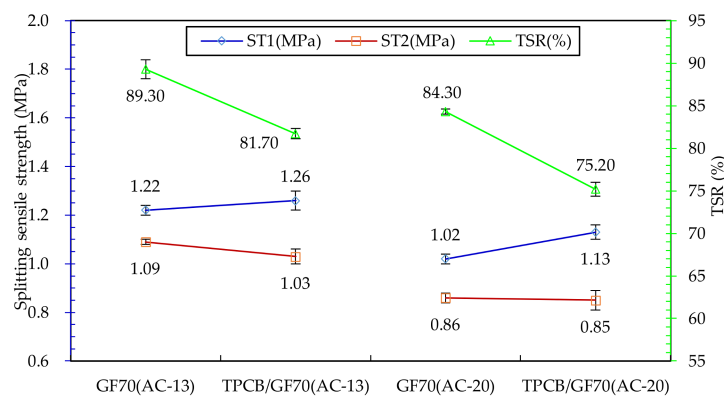


Figure 11. Results of freeze–thaw splitting testing of GF70 and TPCB/GF70 asphalt mixtures.

4. Conclusions

TPCB/GF-70 was prepared by a melt blending method. The characteristics of TPCB such as chemical structure, surface morphology, and particle size distribution were investigated by some modern testing techniques. The physical performance and rheological properties of GF-70 without and with TPCB were studied to investigate TPCB’s effect on the performance of asphalt binders. AHO was used to improve the low-temperature performance of TPCB/GF-70 and its mixtures. The following conclusions can be made:

1. TPCB can decrease the temperature sensitivity and obviously improve the high-temperature performance of asphalt, while a 15% dosage decreases the low-temperature performance of GF-70 within one PG grade.
2. The softening point difference of 15% TPCB-modified asphalt in the segregation test is only 0.7 °C, which shows that TPCB has good compatibility with asphalt.
3. AHO can obviously improve the low-temperature performance and only slightly decreases the high-temperature performance of TPCB/GF-70.

4. With the addition of a 1.2% dosage of AHO and a 0.1% higher oil aggregate ratio, a 15% dosage of TPCB can significantly improve the anti-rutting performance of AC-13 and AC-20 mixtures, as well as improve the low-temperature performance.
5. Both the RMS (higher than 80%) and TSR (higher than 75%) of TPCB and AHO composite modified asphalt mixtures satisfy the requirement of water stability.

Acknowledgments: The authors acknowledge the funding from the Key Laboratory of Road Structure & Material Ministry of Transport, Beijing, China, 100088; and the National Key Scientific Apparatus Development Program of the Ministry of Science and Technology of China (No. 2013YQ160501).

Author Contributions: Shaopeng Wu, Chuangmin Li, and Yuanyuan Li conceived and designed the experiments. Ziran Fan, Yuanyuan Li, and Youwei Gan performed the experiments. Chuangmin Li, Shaopeng Wu, and Yuanyuan Li analyzed the data. Ziran Fan contributed reagents/materials/analysis tools. Ziran Fan, Yuanyuan Li, and Youwei Gan wrote the paper. Shaopeng Wu, Chuangmin Li, Ziran Fan, and Yuanyuan Li designed the software used in the analysis. Aoming Zhang edited the format of this paper. Chuangmin Li and Shaopeng Wu reviewed the paper.

Conflicts of Interest: The authors declare no conflict of interest.

References

1. Uçar, S.; Karagöz, S. Co-pyrolysis of pine nut shells with scrap tires. *Fuel* **2014**, *137*, 85–93. [[CrossRef](#)]
2. González, J.F.; Encinar, J.M.; Canito, J.L.; Rodríguez, J.J. Pyrolysis of automobile tyre waste. Influence of operating variables and kinetics study. *J. Anal. Appl. Pyrolysis* **2001**, *58–59*, 667–683. [[CrossRef](#)]
3. Parthasarathy, P.; Hang, S.C.; Park, H.C.; Hwang, J.G.; Yoo, H.S.; Lee, B.K.; Upadhyay, M. Influence of process conditions on product yield of waste tyre pyrolysis—A review. *Korean J. Chem. Eng.* **2016**, *33*, 1–19. [[CrossRef](#)]
4. Unapumnuak, K.; Lu, M.; Keener, T.C. Carbon Distribution from the Pyrolysis of Tire-Derived Fuels. *Ind. Eng. Chem. Res.* **2006**, *45*, 8757–8764. [[CrossRef](#)]
5. Miranda, M.; Pinto, F.; Gulyurtlu, I.; Cabrita, I. Pyrolysis of rubber tyre wastes: A kinetic study. *Fuel* **2013**, *103*, 542–552. [[CrossRef](#)]
6. Muzenda, E. A comparative review of waste tyre pyrolysis, gasification and liquefaction (PGL) processes. In Proceedings of the International Conference on Chemical Engineering & Advanced Computational Technologies (ICCEACT'2014), Pretoria, South Africa, 24–25 November 2014.
7. Wang, H.; You, Z.; Mills-Beale, J.; Hao, P. Laboratory evaluation on high temperature viscosity and low temperature stiffness of asphalt binder with high percent scrap tire rubber. *Constr. Build. Mater.* **2012**, *26*, 583–590. [[CrossRef](#)]
8. Sienkiewicz, M.; Borzędowska-Labuda, K.; Wojtkiewicz, A.; Janik, H. Development of methods improving storage stability of bitumen modified with ground tire rubber: A review. *Fuel Process. Technol.* **2017**, *159*, 272–279. [[CrossRef](#)]
9. Peralta, J.; Silva, H.M.; Hilliou, L.; Machado, A.V.; Pais, J.; Williams, R.C. Mutual changes in bitumen and rubber related to the production of asphalt rubber binders. *Constr. Build. Mater.* **2012**, *36*, 557–565. [[CrossRef](#)]
10. Roy, C.; Chaala, A.; Darmstadt, H. The vacuum pyrolysis of used tires: End-uses for oil and carbon black products. *J. Anal. Appl. Pyrolysis* **1999**, *51*, 201–221. [[CrossRef](#)]
11. Bhadra, S.; De, P.P.; Mondal, N.; Mukhapadhyaya, R.; Gupta, S.D. Regeneration of carbon black from waste automobile tires. *J. Appl. Polym. Sci.* **2003**, *89*, 465–473. [[CrossRef](#)]
12. Wu, S.; Mo, L.; Shui, Z.; Chen, Z. Investigation of the conductivity of asphalt concrete containing conductive fillers. *Carbon* **2005**, *43*, 1358–1363. [[CrossRef](#)]
13. Wen, S.; Chung, D.D.L. Effects of carbon black on the thermal, mechanical and electrical properties of pitch-matrix composites. *Carbon* **2004**, *42*, 2393–2397. [[CrossRef](#)]
14. Cong, P.; Xu, P.; Chen, S. Effects of carbon black on the anti aging, rheological and conductive properties of SBS/asphalt/carbon black composites. *Constr. Build. Mater.* **2014**, *52*, 306–313. [[CrossRef](#)]
15. Apeageyi, A.K. Laboratory evaluation of antioxidants for asphalt binders. *Constr. Build. Mater.* **2011**, *25*, 47–53. [[CrossRef](#)]
16. Park, T.; Lovell, C.W. *Using Pyrolyzed Carbon Black (PCB) from Waste Tires in Asphalt Pavement (Part 1, Limestone Aggregate)*; Creep Tests: West Lafayette, IN, USA, 1996.

17. Xiao, F.; Amirkhaniyan, A.N.; Amirkhaniyan, S.N. Influence of Carbon Nanoparticles on the Rheological Characteristics of Short-Term Aged Asphalt Binders. *J. Mater. Civ. Eng.* **2011**, *23*, 423–431. [[CrossRef](#)]
18. Liu, X.; Wu, S.; Ye, Q.; Qiu, J.; Li, B. Properties evaluation of asphalt-based composites with graphite and mine powders. *Constr. Build. Mater.* **2008**, *22*, 121–126. [[CrossRef](#)]
19. Gundla, A.; Medina, J.; Gudipudi, P.; Stevens, R.; Salim, R.; Zeiada, W.; Underwood, S. Investigation of Aging in Hydrated Lime and Portland Cement Modified Asphalt Concrete at Multiple Length Scales. *J. Mater. Civ. Eng.* **2015**, *28*, 04015205. [[CrossRef](#)]
20. Kakade, V.B.; Reddy, M.A.; Reddy, K.S. Effect of aging on fatigue performance of hydrated lime modified bituminous mixes. *Constr. Build. Mater.* **2016**, *113*, 1034–1043. [[CrossRef](#)]
21. ASTM International. Standard test method for penetration of bituminous materials. In *Annual Book of ASTM Standards*; American Society for Testing and Materials Annual: Philadelphia, PA, USA, 1992.
22. ASTM International. D36. *Standard Test Method for Softening Point of Bitumen (Ring-and-Ball Apparatus)*; ASTM International: West Conshohocken, PA, USA, 2009.
23. ASTM International. D4402. *Standard Test Method for Viscosity Determination of Asphalt at Elevated Temperatures Using a Rotational Viscometer*; ASTM International: West Conshohocken, PA, USA, 2008.
24. ASTM International. Standard test method for ductility of bituminous materials. In *Annual Book of ASTM Standards*; American Society for Testing and Materials Annual: Philadelphia, PA, USA, 1979.
25. Lu, X.; Isacsson, U. Effect of ageing on bitumen chemistry and rheology. *Constr. Build. Mater.* **2002**, *16*, 15–22. [[CrossRef](#)]
26. Stewart, S.P.; Bell, S.; Mcauley, D. Determination of hydrogen peroxide concentration using a handheld Raman spectrometer: Detection of an explosives precursor. *Forensic Sci. Int.* **2012**, *216*, e5. [[CrossRef](#)] [[PubMed](#)]
27. Elbasuney, S.; El-Sherif, A.F. Complete spectroscopic picture of concealed explosives: Laser induced Raman versus infrared. *TrAC Trends Anal. Chem.* **2016**, *85*, 34–41. [[CrossRef](#)]
28. Cheng, C.H.; Lehmann, J. Ageing of black carbon along a temperature gradient. *Chemosphere* **2009**, *75*, 1021–1027. [[CrossRef](#)] [[PubMed](#)]
29. Cheng, C.H.; Lehmann, J.; Engelhard, M.H. Natural oxidation of black carbon in soils: Changes in molecular form and surface charge along a climosequence. *Geochim. Cosmochim. Acta* **2008**, *72*, 1598–1610. [[CrossRef](#)]
30. Furtado, C.A.; Kim, U.J.; Liu, X.; Gutierrez, H.R.; Chen, G.; Gupta, A.; Eklund, P.C. Raman and IR Spectroscopy of Chemically-Processed Single-Walled Carbon Nanotubes. *J. Am. Chem. Soc.* **2005**, *127*, 15437–15445.
31. China Ministry of Transport. *JTG F40-2004 Technical Specification for Construction of Highway Asphalt Pavements [S]*; China Communications Press: Beijing, China, 2004.
32. Sun, Z.; Yi, J.; Huang, Y.; Feng, D.; Guo, C. Properties of asphalt binder modified by bio-oil derived from waste cooking oil. *Constr. Build. Mater.* **2016**, *102*, 496–504. [[CrossRef](#)]
33. Liang, M.; Xin, X.; Fan, W.; Luo, H.; Wang, X.; Xing, B. Investigation of the rheological properties and storage stability of CR/SBS modified asphalt. *Constr. Build. Mater.* **2015**, *74*, 235–240. [[CrossRef](#)]
34. Rutherford, T.; Wang, Z.; Shu, X.; Huang, B.; Clarke, D. Laboratory investigation into mechanical properties of cement emulsified asphalt mortar. *Constr. Build. Mater.* **2014**, *65*, 76–83. [[CrossRef](#)]
35. Tu, L.; Wu, S.; Liu, G.; Zhou, X.; Ma, S. Effect of the Welan Gum Biopolymer on Rheological Properties and Storage Stability of Bitumens. *J. Test. Eval.* **2016**, *44*, 2211–2218. [[CrossRef](#)]
36. Zeng, W.; Wu, S.; Pang, L.; Sun, Y.; Chen, Z. The Utilization of Graphene Oxide in Traditional Construction Materials: Asphalt. *Materials* **2017**, *10*, 48. [[CrossRef](#)] [[PubMed](#)]
37. Kebria, D.Y.; Moafimadani, S.R.; Goli, Y. Laboratory investigation of the effect of crumb rubber on the characteristics and rheological behaviour of asphalt binder. *Road Mater. Pavement Des.* **2015**, *16*, 946–956. [[CrossRef](#)]
38. Cai, Y.C.; Zheng, Y.X. Experiment Study of Water Stability of Fiber-Reinforced Asphalt Mixture. *Adv. Mater. Res.* **2011**, *243–249*, 710–716. [[CrossRef](#)]

